

Determination of overpressure zone and its mechanism in Baong Formation of the Asahan Field in North Sumatera Basin

Andrea Hasbullah¹, Hendra Amijaya*², and Jarot Setyowiyoto²

¹*STT Migas Cilacap, Jalan Raya Tritih Lor 43, Jeruklegi, Cilacap 53232, Indonesia*

²*Department of Geological Engineering, Faculty of Engineering, Universitas Gadjah Mada, Yogyakarta, Indonesia*

Received: January 24, 2021 | Accepted: August 1, 2023 | Published online: August 20, 2023

ABSTRACT. The Asahan Field is one of the offshore areas in the North Sumatra Basin, which is believed to have an important role in hydrocarbon exploration in the future. The North Sumatra Basin is an area with high overpressure conditions and sometimes is over-predicted, especially in the Baong Formation. This research aims to determine the top and bottom overpressure zones, to know the vertical distribution of overpressure, and to find the main factors causing the overpressure in the Baong Formation. The data used in this study were 5 wells with wireline log data, formation pressure data, test leak, final well reports, mud logs, 29 lines of 2D seismic data, and 1 3D seismic data. This study used the Eaton method to determine pore pressure, whereas the cross-plot wireline log method, the AI (acoustic impedance) inversion method, and the stacking velocity were used to determine pore pressure. The study indicated that the overpressure zone is located in the Baong Formation at 1650–2108 m depth with a pore pressure of around 2891.70–3580 psi. The overpressure is caused by a loading mechanism, namely disequilibrium compaction. The thickness of the formation above the Baong Formation influences this.

Keywords: Baong Formation · North Sumatra basin · overpressure.

1 INTRODUCTION

The North Sumatra Basin has been known as an area with high overpressure conditions (Syaiful et al., 2014). The top overpressure in this basin is mostly located at the top of the Baong Formation. However, overpressure condition in this formation becomes an interesting discussion since there are some difficulties to predict (Syaiful et al., 2014). The cause of overpressure is believed to be related to the rapid deposition or burial of sediment (Azis & Bolt, 1984).

Overpressure mechanisms can be categorized into 3 groups, of which the first group is pressure-related mechanisms such as disequilibrium compaction and tectonic pressure (Swarbrick and Osborne). The two mechanisms

for increasing the volume of the fluids are temperature addition, water discharge due to mineral transformation, hydrocarbon generation, cracking of oil to gas, and gas expansion with uplift. Finally, the fluid movement and buoyancy mechanisms are the hydraulic head, osmosis, buoyancy due to density contrasts, and lateral transfer (Swarbrick & Osborne 1998).

Information on the mechanism of overpressure formation will be very important in accurately predicting the presence of overpressure in a sedimentary basin. Accurate predictions can assist in overcoming drilling operational problems such as casing planning, mud design, blowout prevention design, optimization of well locations, and others. This study will reveal the mechanism that occurred in the studied area, known as Asahan Field (Figure 1, located in the offshore area of the North Sumatera Basin.

*Corresponding author: H. AMIJAYA, Department of Geological Engineering, Universitas Gadjah Mada. Jl. Grafika 2 Yogyakarta, Indonesia. E-mail: hamijaya@ugm.ac.id



FIGURE 1. The location of the Asahan Field in the North Sumatra Basin. Boundaries of the study area are shown in red outline (base map taken from earth.google.com).

2 REGIONAL GEOLOGY

The North Sumatra Basin is located in the northern part of Sumatra, including the coast of North Sumatra. This is a back-arc basin resulting from the subduction of the Indian crust under the Eurasian crust that occurred during the late Eocene – Oligocene (Hakim et al., 2007). This basin is separated from the Central Sumatra Basin by the Asahan Arc. The boundaries of this basin are the Malacca Shelf in the east, the Barisan Mountains in the southwest, the Asahan Arc in the south, and open to the Andaman Sea in the north (Hakim et al., 2007). Initially, the North Sumatra Basin was formed together (Ryacudu et al., 1992) with the West Aceh Basin and the West Sumatra Basin, but the compression structure that forms the Barisan Mountains has separated the North Sumatera Basin from other basins. The average geothermal gradient is $450^{\circ}\text{C}/\text{km}$ with some geothermal gradients greater than $500^{\circ}\text{C}/\text{km}$ and a basin area of 258 km^2 (Ryacudu et al., 1992).

Pertamina divides the Tertiary deposits of the North-East Sumatra Basin into 7 formations, namely the Parapat Formation, Bampo Formation, Belumai Formation, Baong Formation, Keutapang Formation, Seurula Formation, and

Julu Rayeu Formation (Pertamina, 1985). According to a report compiled by Pertamina and BEICIP, the tectonic process of the basin has divided the regional stratigraphy of the North Sumatra Basin in the order from old to young as follows (Pertamina, 1985).

The pre-Tertiary Basement consists of igneous rock, metamorphic rock, carbonate, and Triassic-aged Halobia fossils located out of alignment under the sedimentary rocks above (Pertamina, 1985). Parapat Formation (Early Oligocene) is overlying the basement and consists of coarse sandstones and conglomerates at the bottom of the seta above which there are shale inserts. Regionally the lower part is deposited in a fluvial environment and the upper part in a shallow marine environment (Pertamina, 1985). Bampo Formation (Late Oligocene) is deposited above Parapat Formation. Bampo Formation consists of non-layered black shale associated with thin limestone and carbonate clay layers; these formations are poor in fossils and deposited in a reduced environment.

Belumai Formation (Early Miocene) in the eastern part of this basin developed a formation identical to the Peutu Formation, which devel-

oped in the western and central parts. Belumai Formation consists of Glauconitic sandstones interspersed with shale and limestone (Pertamina, 1985). In the Arun area, the upper part of this formation develops limestone layers of calcarenite and kalsilit with shale intervals. This formation is deposited to neritic in a shallow marine environment (Pertamina, 1985).

Baong Formation was deposited in Middle Miocene to Late Miocene (Pertamina, 1985). The main constituents of this formation are blackish-gray claystone, marl, silt, and sand, and generally rich in fossils of *Orbulina* sp. and *Globigerina* sp., sometimes interspersed with thin layers of sandstones. This formation is deposited in a deep-sea environment (Pertamina, 1985). The Baong Formation above is divided into 3 units (Pertamina, 1985):

- The lower part is dominated by silt and claystone with sandstone and limestone inserts.
- The center (MBS) is dominated by glauconite and clay sandstones with silt inserts and a thin layer of limestone. In this member, several sandstone layers have been proven to contain hydrocarbons, namely the Sembilan sand and the river sand (BRS).
- The upper part is dominated by silt and clay with a sandstone insert and a thin layer of limestone.

Keutapang Formation (Late Miocene) is stratigraphically above Baong Formation and alternates between fine – medium-grained sandstones, shale, clays with limestone inserts, and coal (Pertamina, 1985). This formation is the main layer of hydrocarbon production and is the beginning of the regression cycle, deposited in a deltaic environment to shallow seas. Seurula Formation (Early Pliocene) was deposited above Keutapang Formation and composed of sandstones, flakes, and clay. Compared to the Keutapang Formation, the Seurula Formation is coarser and grain. Many mollusk fragments show shallow or neritic marine deposits. Julu Rayeu Formation (Late Pliocene) is younger than the Seurula Formation and consists of fine sandstones – coarse and loamy, sometimes containing mica and mollusk fragments showing shallow marine deposits – Neritic (see [Figure 2](#)).

3 DATA AND METHODS

The oil and gas data in this study were obtained from the Ministry of Energy and Mineral Resources Data and Information Centre (Pusdatin) provided by PT. Patra Nusa Data. The data consists of 5 wells, namely wells A1, A2, A3, A4, and A5. Each well has complete log data, which are gamma-ray, resistivity, sonic, and density logs, except A5 well, which does not have sonic and density log data. In addition, each well is also equipped with complete pressure test data and well reports, while the leak-off test data is only available at well A5. Other supporting data was seismic data consisting of 29 2D seismic lines where 14 lines lead east to west with an average CDP (common depth point) of 2.02 and 9 lines lead north to south with an average length of CDP of 4.8 km.

In this study, several stages were carried out. We use Eaton's method to predict overpressure (Eaton, 1975). This method usually calculates the pressure below the surface from the loading effect. Overpressure with the loading mechanism is a mechanism that prevents the compacting process from running properly so that the effective stress becomes stagnant even though one of the main stresses continues to rise (Swarbrick and Osborne, 1997). Another method uses a sonic curve inversion to determine the overpressure zone (Manik and Soedaldjo, 1984). Finally, obtain a velocity model using the conventional method (stacking velocity) and acoustic impedance inversion (Etminan 2010).

The hydrostatic pressure, namely with water fluid, is determined according to Zoback (2007), with the hydrostatic gradient of 0.433 psi/ft. The multiplication of sediment density, gravitational acceleration, and depth of the datum is used to calculate the overburden stress. Rock density uses density log data. Calculation of the fracture pressure uses the Matthews and Kelly approach. The fracture pressure is taken when the rock is first fractured, the maximum limit of the rock strength or pore pressure. Then the fracture pressure calculation is validated with the leak of test data (LOT). Overpressure analysis uses hydrostatic pressure data and wireline log data such as sonic logs, density logs, resistivity logs, and neutron logs, which are sup-

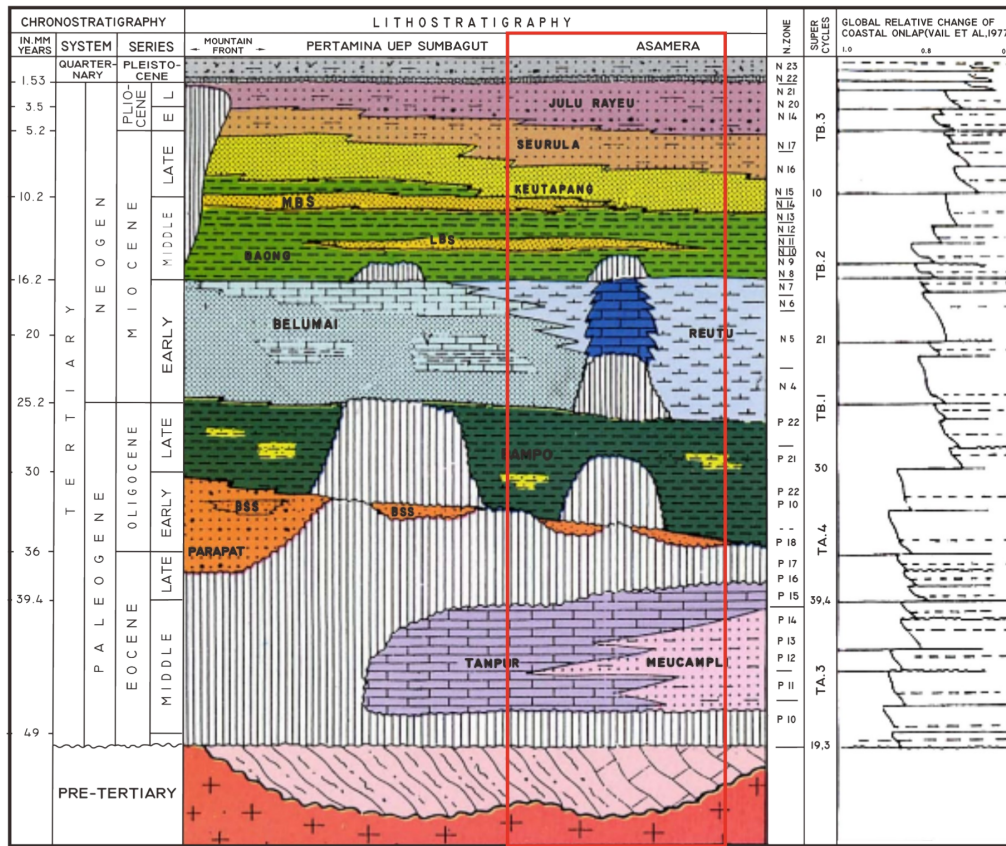


FIGURE 2. Tertiary Stratigraphy of the North Sumatra Basin (Ryucudu et al., 1992).

ported by other data such as pore pressure test data, LOT data, mud log data, final well reports, and seismic data.

The overpressure mechanism was based on analyzing the large change in effective stress using the approach of Terzaghi (1943). The response of the wireline log, cross plot of sonic logs with density logs, and mud log data supported the determination of the mechanism. The overpressure mechanism analysis uses the Dutta plot (Dutta, 2002) and the Bowers plot (Bowers, 2001). Seismic modeling to evaluate the overpressure zone was done by seismic inversion. The process of modeling the pore pressure section starts from the AI inversion with the model-based type. This process obtained the density inversion and velocity inversion models, which were then converted using Hampson Russell software. The final result of the inversion process is the pore pressure section calculated by the Eaton formula using the overburden section and the velocity interval as the input for Eaton parameters. Meanwhile, Petrel software makes the depth structure map (see WesternGeco, 2015).

4 RESULTS AND DISCUSSION

4.1 Lithology and Pressure

The separation of lithology in the well was carried out by plotting the sonic log data, resistivity, density, and porosity against the depth, which aimed to separate the shale and non-shale lithology. Most wells are shale with sandstone intercalation (see Figure 3).

From the pressure analysis in Well A1 (see Figure 4), it can be seen that the pore pressure trend deviates from the normal trend, which should increase with increasing depth, but there is a decrease in the pore pressure value compared to the normal pressure value at 1602 m in the Middle Baong Formation which then increases again at a depth of 1944 m in the Lower Baong Formation. In Well A2, overpressure is seen from the trend of deviating pore pressure from normal pressure, namely at a depth of 1745.87 m, a pressure drop occurs then increases by 2120 m in the Lower Baong Formation. Well A3 indicates a trend of deviating pore pressure from normal pressure, namely at a depth of 1490 m where there is a pressure

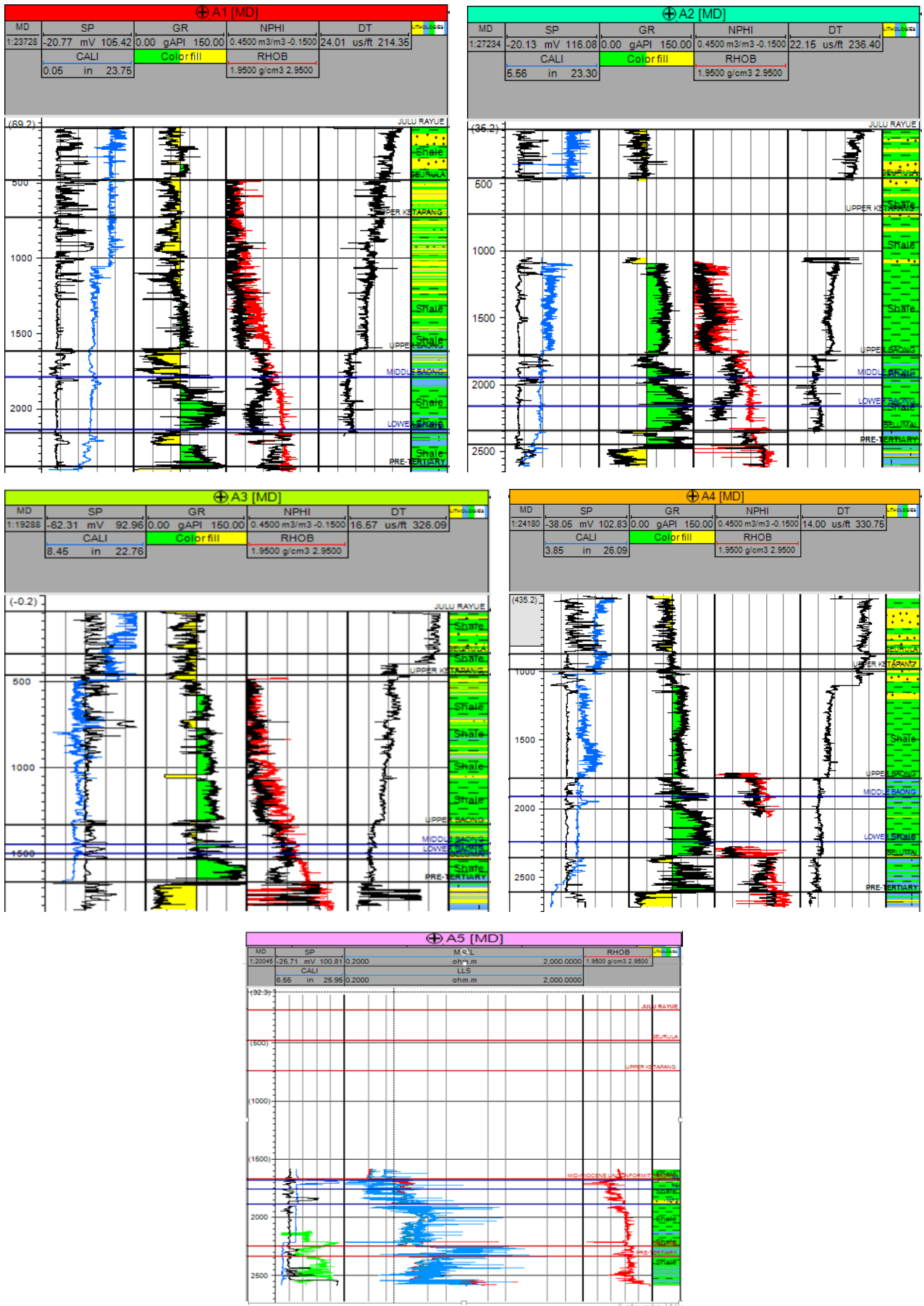


FIGURE 3. Pressure vs depth profile in well A1-A5.

drop and then increased by 1664 m in the Lower Baong Formation.

In Well A4, the position of overpressure is seen from the trend of deviating the pore pressure from normal pressure, namely at a depth of 1775 m, there is a pressure drop then increases by 2356 m in the Baong Formation. Well A5 has incomplete log data; the sonic and density log data used to determine overpressure do not exist. However, the pore pressure plots could still be made using resistance data, but the results were unreliable.

4.2 Overpressure Mechanism

The peaks of the overpressure were analyzed from the sonic log plots and the density logs. In Well A1, determining the overpressure peak from the sonic log can be seen from the deflection of the normal trend and the trend of effective pressure, which tends to be stagnant. Meanwhile, the density log is analyzed by looking at the trend of the density log, which should increase with increasing depth, but in Well A1 shows a stable trend pattern. Furthermore, the combination of sonic log data and density coupled with pressure data plots shows the peak of overpressure, which shows the beginning of overpressure in Well A1 at a depth of 2012 m in the Lower Baong Formation. Also, the combination of log and pressure data plots indicates a loading mechanism in Well A1.

In Well A1, the Dutta plot and Bowers are used, namely the plot between the density log and the sonic log, to determine the level of the rock diagenesis (Figure 5 and Figure 6). From the result of the research data, it is obtained that the data trend follows the illite trend at a depth of 1000–2000 m, then moves to the smectite trend at 2000–2164 m depth. This means that in Well A1, the cause of the overpressure mechanism is the loading mechanism. Meanwhile, the Bowers plot using velocity and density log plots shows that the data follows the upper bound trend starting from a depth of 1000–2000 m and at depths 2000–2164 following the lower bound trend. So that it can be said that the cause of the overpressure in Well A1 is the loading mechanism because there is no indication of a plot reversal trend.

4.3 Overpressure Distribution from Seismic

Velocity and density inversion sections are obtained based on the qualitative interpretation of the inverted seismic data with acoustic impedance. Then the cross-section is converted to an inversion gradient overburden section, which continues to be an inversion pore pressure section using Eaton's equation. The pore pressure results show the same results as the quantitative calculation using well data to calculate the pore pressure in each well. Figure 7 shows the result of the above-mentioned seismic inversion process.

Furthermore, it can be seen from the color bar that the pore pressure inversion section shows an increase in pressure which is marked by a change in color from yellow (12 ppg) to reddish yellow (14 ppg) from the Keutapang Formation to the Baong Formation. This is because the Keutapang Formation is a source of hydrocarbons where the lithology is composed of sandstone, claystone, and limestone inserts and deposited in deltaic and shallow marine environments. While the Baong Formation is dominated by claystone with sandstone inserts deposited in the deep sea. The color change indicates changes in lithology from rocks composed of sandstone in the Keutapang formation to rocks dominated by claystone. This shows the cause of the increase in pore pressure values because the Baong formation has a good seal capacity.

5 CONCLUSION

1. The results of the pore pressure prediction in the well show a high pore pressure value in the shale zone caused by overpressure in the study area. Based on pore pressure calculations, the overpressure zone is located at a depth of approximately 1650–2108 m with a pore pressure of around 2891.70–3580 psi in the Baong Formation.
2. Calculating pore pressure using well data helps to determine the vertical pore pressure distribution, which results in the peak of overpressure. The overpressure distribution can be observed horizontally from the seismic inversion and interval velocity distribution. The pattern of overpressure

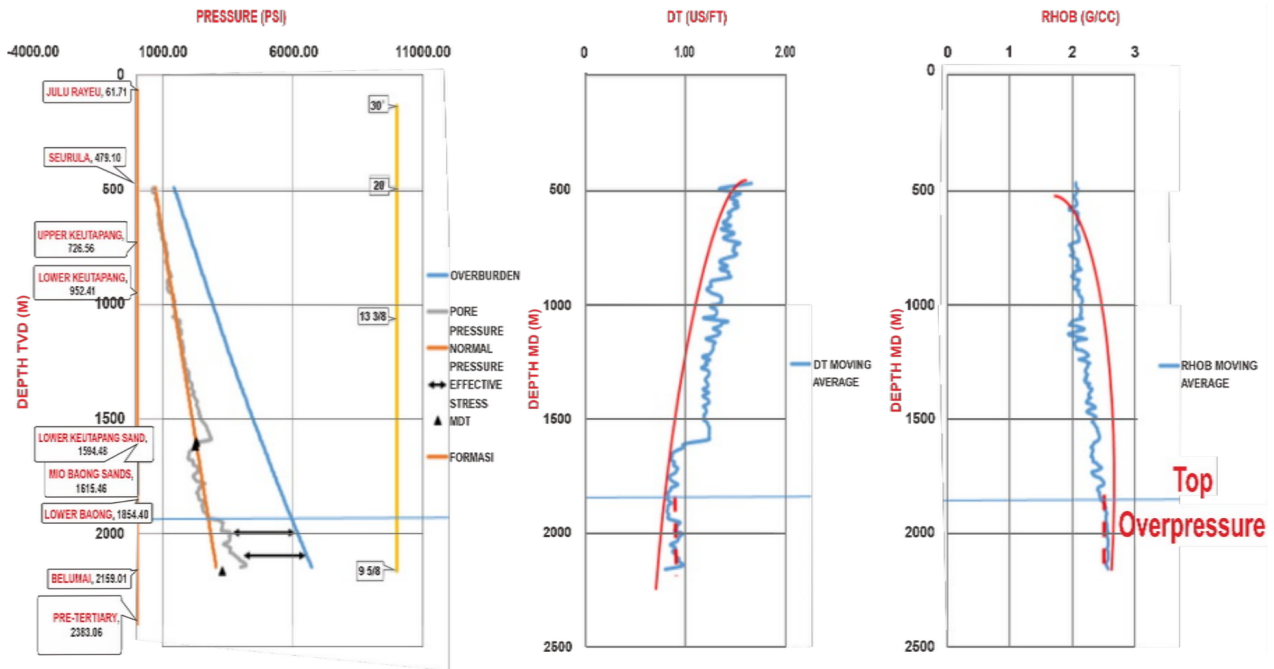


FIGURE 4. Determination of the overpressure peak of well A1.

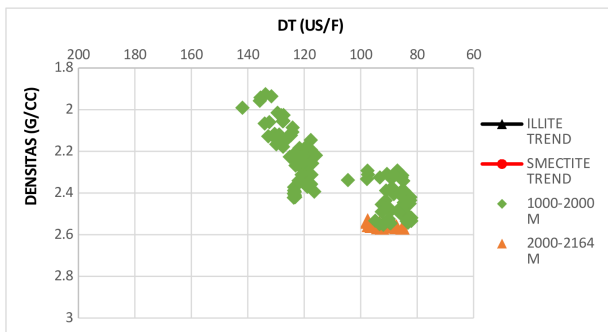


FIGURE 5. Cross-plot on Dutta plot based on Sonic vs Density of well A1.

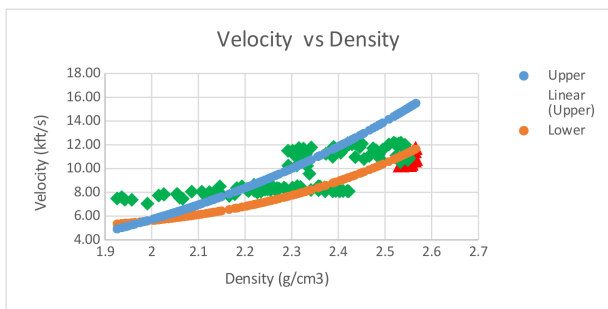


FIGURE 6. Cross-plot on Bowers plot based on Velocity vs Density of well A1.

in the study area follows the shale thickness of the Baong formation structurally.

3. The mechanism that causes overpressure in the study area is the loading mechanism, namely disequilibrium compaction. This is influenced by the thickness of the formation above the thick overpressure zone, which is dominated by shale.

Acknowledgements The authors wish to thank PT. Patra Nusa Data for providing data used in this study.

REFERENCES

Azis, A., & Bolt, L.H. (1984). Occurrence and detection of abnormal pressure from geological and drilling data, North Sumatra Basin. *Proceedings Indonesian Petroleum Association 13th Annual Convention*, 195-220.

Bowers, G.L. (2001). Determining an appropriate pore-pressure estimation strategy. *Offshore Technology Conference*, paper OTC 13042, 2-4.

Dutta, N.C. (2002). Deepwater geohazard prediction using prestack inversion of large offset P-wave data and rock model. *The Leading Edge*, 21, 193-198.

Eaton, B.A. (1975). The equation for geopressure prediction from well logs. SPE, Paper No. 5544, 2-4.

Etmnan, M. (2010). Estimation of formation pressure using velocity inversion result of seismic data in Sefid-Zakhor anticline, M.Sc. thesis [unpub-

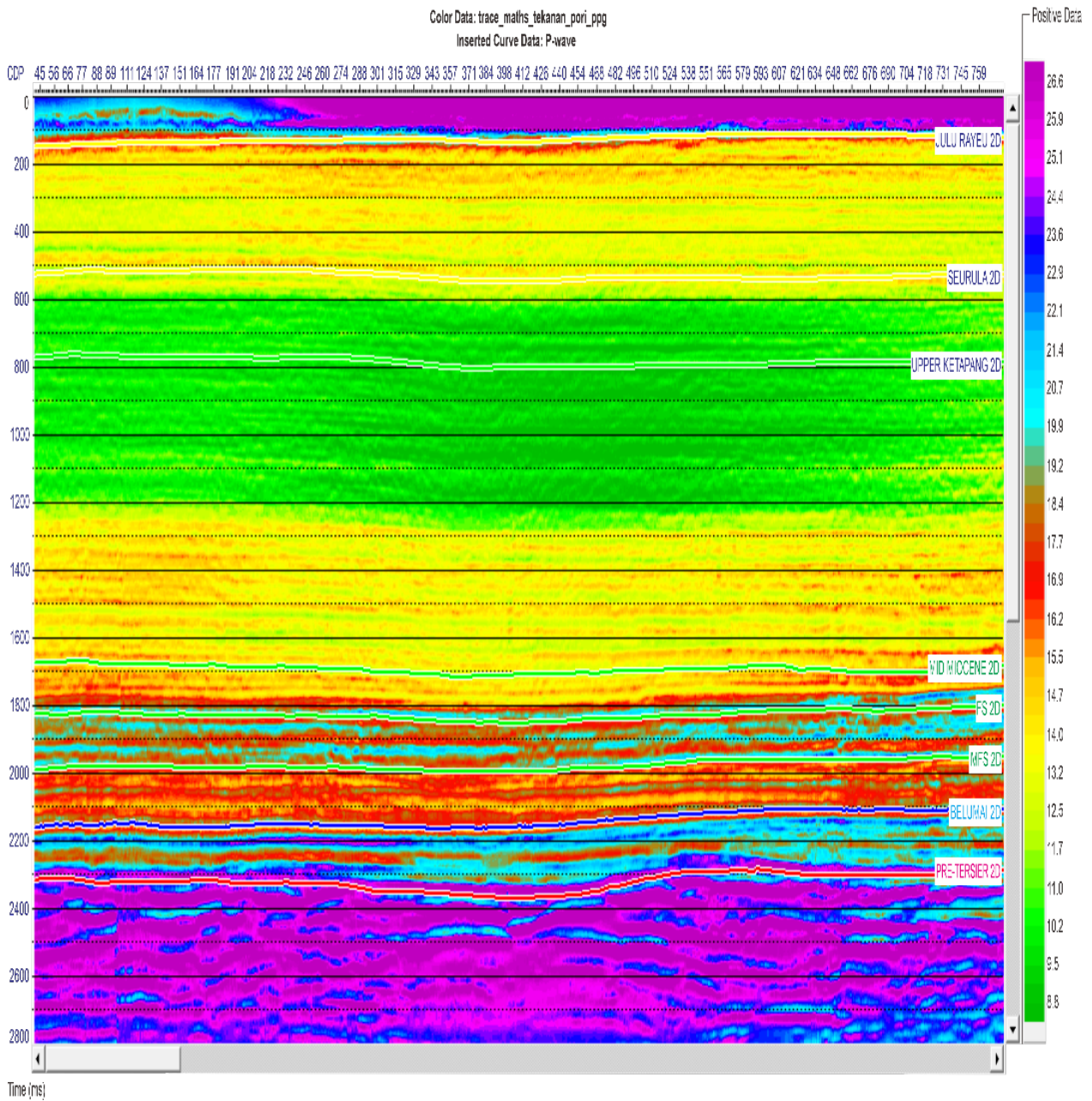


FIGURE 7. The pore pressure section in ppg units indicates increasing pressure in the upper part of the Baong Formation, shown by the color change from reddish yellow (Keutapang Formation) to red-blue (Upper Baong) and back to red (Mid Baong).

- lished], Tehran University. Department of Mining Engineering, 291 p.
- Hakim, M.R., Faris, M., & Yordan, M. (2007). Hydrocarbon Play in North Sumatra Basin and Sequence Stratigraphy Application on Keutapang Reservoir Formation Based on Well Logs Data. *Proceedings Indonesian Petroleum Association 30th Annual Convention*, SG 006.
- Manik, P., & Soedaljo, P.A. (1984). Prediction of abnormal pressure based on seismic data. A case study of exploration well drilling in Pertamina UEP I and UEP II work areas. *Proceedings Indonesian Petroleum Association 13th Annual Convention*, 461-505.
- Matthews, W.R., & Kelly, J. (1967). How to Predict Formation Pressure and Fracture Gradient. *Oil and Gas Journal*, 65, 92-1066.
- Pertamina-Beicip (1985). *Petroleum potential of Western Indonesia*. [Unpublished Technical Report].
- Ryacudu, R., Djaafar, R. & Gutomo, A., (1992). Wrench faulting and its implication for hydrocarbon accumulation in the Kuala Simpang area – North Sumatra Basin. *Proceedings Indonesian Petroleum Association 21th Annual Convention*, 93-116.
- Swarbrick, R.E. (1997). Characteristics of overpressured basins and influence of overpressure on the petroleum system. In: Howes, J.V.C. & Noble, R.A. (eds.), *Indonesian Petroleum Association, Proceedings of the Petroleum Systems of SE Asia and Australasia Conference*, 859-865.
- Swarbrick, R.E., & Osborne, M.J. (1998). *Mechanisms that generate abnormal pressures: an overview*. In: Law, B.E., Ulmishek, G.F. & Slavin, V.I. (eds.) *Abnormal Pressures in Hydrocarbon Environments*. AAPG Memoir 70, Tulsa, 13-34.
- Syaiful, M., (2014). Shifting of compaction trend in the North Sumatra Basin and its implication to overpressure estimation in the North Sumatra Basin. *Proceedings Indonesian Petroleum Association 38th Annual Convention*, G-358.
- Terzaghi, K., & Peck, R.B., (1967), *Soil Mechanics in Engineering Practice*. 2nd Edition: New York, John Wiley & Sons, 729 p.
- WesternGeco Multi Client Services, (2018). Petrel, Schlumberger.
- Zoback, M. D., (2007). *Reservoir Geomechanics*. Cambridge University Press, Cambridge, 445 p.